

DETERMINATION OF V_{cb} AND V_{ub}

Revised March 2008 by R. Kowalewski (Univ. of Victoria, Canada) and T. Mannel (Univ. of Siegen, Germany).

INTRODUCTION

Precision determinations of $|V_{ub}|$ and $|V_{cb}|$ are central to testing the CKM sector of the Standard Model, and complement the measurements of CP asymmetries in B decays. The length of the side of the unitarity triangle opposite the well-measured angle β is proportional to the ratio $|V_{ub}|/|V_{cb}|$, making its determination a high priority of the heavy-flavor physics program.

The semileptonic transitions $b \rightarrow c\ell\bar{\nu}_\ell$ and $b \rightarrow u\ell\bar{\nu}_\ell$ provide two avenues for determining these CKM matrix elements, namely through inclusive and exclusive final states. The experimental and theoretical techniques underlying these two avenues are independent, providing a crucial cross-check on our understanding. Significant progress has been made in both approaches since the previous review [1].

The theory underlying the determination of $|V_{qb}|$ is mature. The theoretical approaches all use the fact that the mass m_b of the b quark is large compared to the scale Λ_{QCD} that determines low-energy hadronic physics. The basis for precise calculations is a systematic expansion in powers of Λ_{QCD}/m_b , where effective-field-theory methods are used to separate non-perturbative from perturbative contributions. The expansion in Λ_{QCD}/m_b and α_s works well enough to enable a precision determination of $|V_{cb}|$ and $|V_{ub}|$ in semileptonic decays.

The large data samples available at the B factories have opened up new possibilities experimentally. Analyses where one B meson from an $\Upsilon(4S)$ decay is fully reconstructed allow a recoiling semileptonic B decay to be studied with higher purity than was previously possible. Improved knowledge of $\bar{B} \rightarrow X_c\ell\bar{\nu}_\ell$ decays allows partial rates for $\bar{B} \rightarrow X_u\ell\bar{\nu}_\ell$ transitions to be measured in regions previously considered inaccessible, increasing the acceptance for $\bar{B} \rightarrow X_u\ell\bar{\nu}_\ell$ transitions and reducing theoretical uncertainties.

At present, the inclusive determinations of both $|V_{cb}|$ and $|V_{ub}|$ are more precise than the corresponding exclusive determinations. Improvement of the exclusive determinations remains an important goal, and future progress, in particular in lattice QCD, may provide this.

Throughout this review the numerical results quoted are based on the methods of the Heavy Flavor Averaging Group [2].

DETERMINATION OF V_{cb}

Summary: The determination of $|V_{cb}|$ from $\bar{B} \rightarrow D^* \ell \bar{\nu}_\ell$ decays is currently at a relative precision of about 3%. The main limitation is the knowledge of the form factor near the maximum momentum transfer to the leptons. Further progress from lattice calculations of the form factors is needed to improve the precision. For the $\bar{B} \rightarrow D \ell \bar{\nu}_\ell$ channel, experimental measurements must also be improved.

Determinations of $|V_{cb}|$ from inclusive decays are currently below 2% relative uncertainty. The limitations arise mainly from our ignorance of higher order perturbative and non-perturbative corrections.

The values obtained from inclusive and exclusive determinations are currently only marginally consistent with each other:

$$|V_{cb}| = (41.6 \pm 0.6) \times 10^{-3} \text{ (inclusive)} \quad (1)$$

$$|V_{cb}| = (38.6 \pm 1.3) \times 10^{-3} \text{ (exclusive)}. \quad (2)$$

An average of the above gives $|V_{cb}| = (41.2 \pm 0.5) \times 10^{-3}$, with $P(\chi^2) = 0.03$. Scaling the error by $\sqrt{\chi^2/\text{ndf}} = 2.1$ we quote

$$|V_{cb}| = (41.2 \pm 1.1) \times 10^{-3}. \quad (3)$$

$|V_{cb}|$ from exclusive decays

Exclusive determinations of $|V_{cb}|$ are based on a study of semileptonic B decays into the ground-state charmed mesons D and D^* . The main uncertainties in this approach stem from our ignorance of the form factors describing the $B \rightarrow D$ and $B \rightarrow D^*$ transitions. However, in the limit of infinite bottom- and charm-quark masses, only a single form factor appears, the

Isgur-Wise function [3], which depends on the product of the four-velocities v and v' of the initial- and final-state hadrons.

The extraction of $|V_{cb}|$ is based on the distribution of the variable $w \equiv v \cdot v'$, which corresponds to the energy of the final-state $D^{(*)}$ meson in the rest frame of the decay. Heavy Quark Symmetry (HQS) [3,4] predicts the normalization of the rate at $w = 1$, the point of maximum momentum transfer to the leptons, and $|V_{cb}|$ is obtained from an extrapolation of the measured spectrum to $w = 1$.

A precise determination requires corrections to the HQS prediction for the normalization, as well as some information on the slope of the form factors near the point $w = 1$, since the phase space vanishes there. The corrections to the HQS prediction due to finite quark masses are given in terms of the symmetry-breaking parameter

$$\frac{1}{\mu} = \frac{1}{m_c} - \frac{1}{m_b},$$

which is essentially $1/m_c$ for realistic quark masses. HQS ensures that those matrix elements that correspond to the currents that generate the HQS are normalized at $w = 1$; as a result, some of the form factors either vanish or are normalized at $w = 1$. Due to Luke's Theorem [5] (which is an application of the Ademollo-Gatto theorem [6] to heavy quarks), the leading correction to those form factors normalized due to HQS is quadratic in $1/\mu$, while for the form factors that vanish in the infinite mass limit, the corrections are in general linear in $1/m_c$ and $1/m_b$. Thus we have, using the definitions as in Eq. (2.84) of Ref. 7,

$$\begin{aligned} h_i(1) &= 1 + \mathcal{O}(1/\mu^2) && \text{for } i = +, V, A_1, A_3, \\ h_i(1) &= \mathcal{O}(1/m_c, 1/m_b) && \text{for } i = -, A_2. \end{aligned} \quad (4)$$

In addition to these corrections, there are perturbatively calculable radiative corrections from QCD and QED, which will be discussed in the relevant sections. Both - radiative corrections as well as $1/m$ corrections - are considered in the framework of Heavy Quark Effective Theory (HQET) [8], which provides for a systematic expansion.

$\overline{B} \rightarrow D^* \ell \overline{\nu}_\ell$

The decay rate for $\overline{B} \rightarrow D^* \ell \overline{\nu}_\ell$ is given by

$$\frac{d\Gamma}{dw}(\overline{B} \rightarrow D^* \ell \overline{\nu}_\ell) = \frac{G_F^2}{48\pi^3} |V_{cb}|^2 m_{D^*}^3 (w^2 - 1)^{1/2} P(w) (\mathcal{F}(w))^2, \quad (5)$$

where $P(w)$ is a phase-space factor with $P(1) = 12(m_B - m_{D^*})^2$, and $\mathcal{F}(w)$ is dominated by the axial vector form factor h_{A_1} as $w \rightarrow 1$. In the infinite-mass limit, the HQS normalization gives $\mathcal{F}(1) = 1$.

The form factor $\mathcal{F}(w)$ must be parametrized to perform an extrapolation to the zero-recoil point. A frequently used one-parameter form motivated by analyticity and unitarity is [9,10]

$$\mathcal{F}(w) = \eta_{\text{QED}} \eta_A \left[1 + \delta_{1/m^2} + \dots \right] \left[1 - 8\rho_{A_1}^2 z + (53\rho_{A_1}^2 - 15)z^2 - (231\rho_{A_1}^2 - 91)z^3 \right], \quad (6)$$

with $z = (\sqrt{w+1} - \sqrt{2})/(\sqrt{w+1} + \sqrt{2})$ originating from a conformal transformation. The parameter $\rho_{A_1}^2$ is the slope of the form factor at $w = 1$. The η_{QED} and η_A factors are the QED [11] and QCD [12] short-distance radiative corrections

$$\eta_{\text{QED}} = 1.007, \quad \eta_A = 0.960 \pm 0.007, \quad (7)$$

and δ_{1/m^2} comes from non-perturbative $1/m^2$ corrections.

Recently, lattice simulations which include effects from finite quark masses have been used to calculate the deviation of $\mathcal{F}(1)$ from unity. The value quoted from these calculations, multiplied by η_{QED} , is

$$\mathcal{F}(1) = 0.930 \pm 0.023, \quad (8)$$

where the errors quoted in Ref. 13 have been added in quadrature. This value is compatible with estimates based on non-lattice methods.

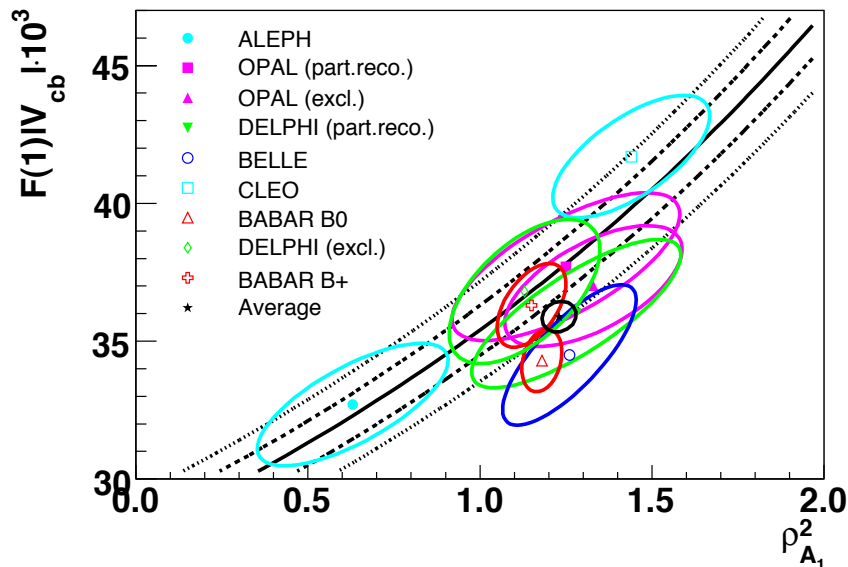


Figure 1: Measurements of $|V_{cb}|\mathcal{F}(1)$ vs. $\rho_{A_1}^2$ are shown as $\Delta\chi^2 = 1$ ellipses. The curves (central value, $\pm 1\sigma$ and $\pm 2\sigma$) correspond to the measurement of the total rate $\Gamma(\bar{B} \rightarrow D^*\ell\bar{\nu}_\ell)$ from Ref. 22.

Many experiments [14–21] have measured the differential rate as a function of w . Fig. 1 shows corresponding values of $|V_{cb}|\mathcal{F}(1)$ and $\rho_{A_1}^2$ (as defined in Ref. 10). These measurements have been updated using more precise values [20] for the form factor ratios $R_1 \propto A_2/A_1$ and $R_2 \propto V/A_1$. The leading sources of uncertainty on $|V_{cb}|\mathcal{F}(1)$ are due to detection efficiencies and $D^{(*)}$ decay branching fractions, while for ρ^2 the uncertainties in R_1 and R_2 still dominate. Related measurements [22,23] of $\Gamma(\bar{B} \rightarrow D^*\ell\bar{\nu}_\ell)$ using samples at the $\Upsilon(4S)$, in which the opposite B is fully reconstructed, have recently been made. These use the measured missing mass squared to isolate signal decays, and have very little sensitivity to the form factor slope. The curves corresponding to constant total rate are shown in Fig. 1.

The confidence level of the average[†] based on the measurements in Fig. 1 is $\sim 2.6\%$. In light of the marginal consistency, we choose to rescale the errors by $\sqrt{\chi^2/\text{ndf}} = 1.5$ to find $|V_{cb}|\mathcal{F}(1) = (35.9 \pm 0.8) \times 10^{-3}$. Along with the value given above for $\mathcal{F}(1)$ this yields

$$|V_{cb}| = (38.6 \pm 0.9_{\text{exp}} \pm 1.0_{\text{theo}}) \times 10^{-3}. \quad (9)$$

$\overline{B} \rightarrow D\ell\overline{\nu}_\ell$

The differential rate for $\overline{B} \rightarrow D\ell\overline{\nu}_\ell$ is given by

$$\begin{aligned} \frac{d\Gamma}{dw}(\overline{B} \rightarrow D\ell\overline{\nu}_\ell) = \\ \frac{G_F^2}{48\pi^3} |V_{cb}|^2 (m_B + m_D)^2 m_D^3 (w^2 - 1)^{3/2} (\mathcal{G}(w))^2. \end{aligned} \quad (10)$$

The form factor is

$$\mathcal{G}(w) = h_+(w) - \frac{m_B - m_D}{m_B + m_D} h_-(w), \quad (11)$$

where h_+ is normalized due to HQS and h_- vanishes in the heavy mass limit. Thus,

$$\mathcal{G}(1) = 1 + \mathcal{O}\left(\frac{m_B - m_D}{m_B + m_D} \frac{1}{m_c}\right), \quad (12)$$

and the corrections to the HQET predictions are parametrically larger than was the case for $\overline{B} \rightarrow D^*\ell\overline{\nu}_\ell$.

In order to get a more precise prediction for the form factor $\mathcal{G}(1)$, the heavy quark limit can be supplemented by additional assumptions. It has been argued in Ref. 24 that in a limit in which the kinetic energy μ_π^2 is equal to the chromomagnetic moment μ_G^2 (these quantities are discussed below in more detail), one may obtain the value

$$\mathcal{G}(1) = 1.04 \pm 0.01_{\text{power}} \pm 0.01_{\text{pert}}. \quad (13)$$

[†] Note that the average does not include the BaBar B^+ measurement, nor the measurement of $\Gamma(\overline{B} \rightarrow D^*\ell\overline{\nu}_\ell)$ shown in the figure, pending a full treatment of their correlations with the BaBar B^0 measurement.

Recently, lattice calculations including effects beyond the heavy mass limit have become available, and hence the fact that deviations from the HQET predictions are parametrically larger than in the case $\bar{B} \rightarrow D^* \ell \bar{\nu}_\ell$ is irrelevant. These unquenched calculations quote a (preliminary) value [25]

$$\mathcal{G}(1) = 1.074 \pm 0.018 \pm 0.016 , \quad (14)$$

which has an error comparable to the one quoted for $\mathcal{F}(1)$, although some uncertainties have not been taken into account.

The measurements [14,26,27] of $|V_{cb}| \mathcal{G}(1)$ result in an average value $|V_{cb}| \mathcal{G}(1) = (42.3 \pm 4.5) \times 10^{-3}$. Using the value given in Eq. (14) for $\mathcal{G}(1)$, accounting for the QED correction and conservatively adding the theory uncertainties linearly results in

$$|V_{cb}| = (39.4 \pm 4.2 \pm 1.3) \times 10^{-3} , \quad (15)$$

where the first uncertainty is from experiment and the second from theory.

Measuring the differential rate at $w = 1$ is more difficult in $\bar{B} \rightarrow D \ell \bar{\nu}_\ell$ decays than in $\bar{B} \rightarrow D^* \ell \bar{\nu}_\ell$ decays, since the rate is smaller and the background from mis-reconstructed $\bar{B} \rightarrow D^* \ell \bar{\nu}_\ell$ decays is significant; this is reflected in the larger experimental uncertainty. The B factories can address these limitations by studying decays recoiling against fully reconstructed B mesons, or doing a global fit to $\bar{B} \rightarrow X_c \ell \bar{\nu}_\ell$ decays. Theoretical input on the shape of the w spectrum in $\bar{B} \rightarrow D \ell \bar{\nu}_\ell$ is valuable, as precise measurements of the total rate are easier; a recent measurement [22] of $\mathcal{B}(\bar{B} \rightarrow D \ell \bar{\nu}_\ell)$ has an uncertainty of $\sim 5\%$.

Prospects for Lattice determinations of the $B \rightarrow D^{(*)}$ form factors

Lattice determinations of the $B \rightarrow D^{(*)}$ form factors have improved significantly over the last few years. The key for the improvements [13,28] is a set of double-ratios, constructed so that all uncertainties scale with the deviation of the form factor from unity. In combination with the possibility to perform unquenched calculations, *i.e.*, calculations with realistic sea quarks, these double ratios yield quite precise predictions for form factors.

The remaining uncertainties are due to the chiral extrapolation from the light quark masses used in the numerical lattice computation to realistic up and down quark masses, and to discretization errors. These sources of uncertainty will be reduced with larger lattice sizes and smaller lattice spacings. The total uncertainty in the lattice values of $\mathcal{F}(1)$ and $\mathcal{G}(1)$ obtained from this method will be 2-3%. However, in the light of the current $> 2\sigma$ tension between inclusive and exclusive $|V_{cb}|$, a revision of the systematic uncertainties becomes important.

In addition to the lattice calculations of form factor normalizations, first results for the w dependence of the form factors are available [29]. While these first results are still in the quenched approximation, one can expect further calculations of form factor shapes in the near future, which will allow comparisons with the experimentally measured shapes.

Decays to Excited D Meson States

Above the ground state D and D^* mesons lie four positive-parity states with one unit of orbital angular momentum, generically denoted as D^{**} . In the heavy mass limit, they form two spin-symmetry doublets with $j_\ell = 1/2$ and $j_\ell = 3/2$, where j_ℓ is the total angular momentum of the light degrees of freedom. The doublet with $j_\ell = 3/2$ is expected to be narrow, while the states with $j_\ell = 1/2$ should be broad, consistent with experimental measurements. Furthermore, one expects that in the heavy mass limit $\Gamma(B \rightarrow D^{**}(j_\ell = 3/2)\ell\bar{\nu}) \gg \Gamma(B \rightarrow D^{**}(j_\ell = 1/2)\ell\bar{\nu})$. A recent measurement indicates this expectation may be violated [23]. If this result is confirmed, it may indicate substantial mixing between the two spin-symmetry doublets, which can occur due to terms of order $1/m_c$. However, the impact on the exclusive V_{cb} determination is expected to be small, since the zero-recoil point is protected against corrections of order $1/m_c$ by Luke's theorem.

$|V_{cb}|$ from inclusive decays

At present, the most precise determinations of $|V_{cb}|$ come from inclusive decays. The method is based on a measurement of the total semileptonic decay rate, together with the leptonic energy and the hadronic invariant mass spectra of inclusive semileptonic decays. The total decay rate can be calculated

quite reliably in terms of non-perturbative parameters that can be extracted from the information contained in the spectra.

Inclusive semileptonic rate

The theoretical foundation for the calculation of the total semileptonic rate is the Operator Product Expansion (OPE), which yields the Heavy Quark Expansion (HQE), a systematic expansion in inverse powers of the b -quark mass [30,31]. The validity of the OPE is proven in the deep euclidean region for the momenta (which is satisfied, *e.g.*, in deep inelastic scattering), but its application to heavy quark decays requires a continuation to time-like momenta $p_B^2 = M_B^2$, where possible contributions which are exponentially damped in the euclidean region could become oscillatory. The validity of the OPE for inclusive decays is equivalent to the assumption of parton-hadron duality, hereafter referred to simply as duality, and possible oscillatory contributions would be an indication of duality violation.

Duality-violating effects are hard to quantify. In practice, they would appear as unnaturally large coefficients of higher order terms in the $1/m$ expansion [32]. The description of ~ 60 measurements in terms of ~ 6 free parameters in global fits to $\overline{B} \rightarrow X_c \ell \overline{\nu}_\ell$ decays provides a non-trivial testing ground for the HQE predictions. Present fits include terms up to order $1/m_b^3$, the coefficients of which have sizes as expected *a priori* by theory. The consistency of the data with these OPE fits will be discussed later; no indication is found that terms of order $1/m_b^4$ or higher are large, and there is no evidence for duality violations in the data. Thus duality or, likewise, the validity of the OPE, is assumed in the analysis, and no further uncertainty is assigned to potential duality violations.

The OPE result for the total rate can be written schematically (the details of the expression can be found, *e.g.*, in Ref. 33) as

$$\Gamma = |V_{cb}|^2 \hat{\Gamma}_0 m_b^5(\mu) (1 + A_{ew}) A^{\text{pert}}(r, \mu) \times \left[z_0(r) + z_2(r) \left(\frac{\mu_\pi^2}{m_b^2}, \frac{\mu_G^2}{m_b^2} \right) + z_3(r) \left(\frac{\rho_D^3}{m_b^3}, \frac{\rho_{\text{LS}}^3}{m_b^3} \right) + z_4(r) \left(\frac{s_i}{m_b^4} \right) + \dots \right], \quad (16)$$

where A_{ew} denotes the electroweak, and $A^{\text{pert}}(r, \mu)$ the QCD radiative corrections, r is the ratio m_c/m_b , and the z_i are known phase-space functions.

This expression is known up to order $1/m_b^4$, where the terms of order $1/m_b^3$ and $1/m_b^4$ have been computed only at tree level [34–36]. The leading term is the parton model, which is known completely to order α_s , and the terms of order $\alpha_s^2\beta_0$ (where β_0 is the first coefficient of the QCD β function, $\beta_0 = (33 - 2n_f)/3$) have been included by the usual BLM procedure [33,37]. Furthermore, the corrections of order $\alpha_s\mu_\pi^2/m_b^2$ have been computed recently [38].

The HQE parameters are given in terms of forward matrix elements by

$$\begin{aligned}\bar{\Lambda} &= M_B - m_b \\ \mu_\pi^2 &= -\langle B|\bar{b}(iD_\perp)^2b|B\rangle \\ \mu_G^2 &= \langle B|\bar{b}(iD_\perp^\mu)(iD_\perp^\nu)\sigma_{\mu\nu}b|B\rangle \\ \rho_D^3 &= \langle B|\bar{b}(iD_{\perp\mu})(ivD)(iD_\perp^\nu)b|B\rangle \\ \rho_{\text{LS}}^3 &= \langle B|\bar{b}(iD_\perp^\mu)(ivD)(iD_\perp^\nu)\sigma_{\mu\nu}b|B\rangle ,\end{aligned}\quad (17)$$

while the five hadronic parameters s_i of the order $1/m_b^4$ can be found in Ref. 35; these have not yet been included in the fits. The non-perturbative matrix elements depend on the renormalization scale μ , on the chosen renormalization scheme, and on the quark mass m_b . The rates and the spectra depend strongly on m_b (or equivalently on $\bar{\Lambda}$), which makes the discussion of renormalization issues mandatory.

Using the pole-mass definition for the heavy quark masses, it is well known that the corresponding perturbative series of decay rates does not converge very well, making a precision determination of $|V_{cb}|$ in such a scheme impossible. The solution to this problem is to choose an appropriate “short-distance” mass definition. Frequently used mass definitions are the kinetic scheme [39,40], or the 1S scheme [41]. Both of these schemes have been applied to semi-leptonic $b \rightarrow c$ transitions, yielding comparable results and uncertainties.

The 1S scheme eliminates the b quark pole mass by relating it to the perturbative expression for the mass of the 1S state

of the \mathcal{Y} system. The physical mass of the $\mathcal{Y}(1S)$ contains non-perturbative contributions, which have been estimated in Ref. 42. These non-perturbative contributions are small; nevertheless, the best determination of the b quark mass in the 1S scheme is obtained from sum rules for $e^+e^- \rightarrow b\bar{b}$.

Alternatively one may use a short-distance mass definition such as the $\overline{\text{MS}}$ mass $m_b^{\overline{\text{MS}}}(m_b)$. However, it has been argued that the scale m_b is unnaturally high for B decays, while for smaller scales $\mu \sim 1 \text{ GeV}$ $m_b^{\overline{\text{MS}}}(\mu)$ is under poor control. For this reason, the so-called “kinetic mass” $m_b^{\text{kin}}(\mu)$ has been proposed. It is the mass entering the non-relativistic expression for the kinetic energy of a heavy quark, and is defined using heavy quark sum rules [40].

The HQE parameters also depend on the renormalization scale and scheme. The matrix elements given in Eq. (17) are defined with the full QCD fields and states, which is the definition frequently used in the kinetic scheme. Sometimes slightly different parameters λ_1 and λ_2 are used, which are defined in the infinite mass limit. The relation between these parameters is

$$\begin{aligned} \overline{\Lambda}_{\text{HQET}} &= \lim_{m_b \rightarrow \infty} \overline{\Lambda}, & -\lambda_1 &= \lim_{m_b \rightarrow \infty} \mu_\pi^2 \\ \lambda_2 &= \lim_{m_b \rightarrow \infty} \mu_G^2, & \rho_1 &= \lim_{m_b \rightarrow \infty} \rho_D^3 \\ \rho_2 &= \lim_{m_b \rightarrow \infty} \rho_{LS}^3. \end{aligned}$$

Defining the kinetic energy and the chromomagnetic moment in the infinite-mass limit (as, *e.g.*, in the 1S scheme) requires that $1/m_b$ corrections to the matrix elements defined in Eq. (17) be taken into account once one goes beyond order $1/m_b^2$. As a result, additional quantities $\mathcal{T}_1 \cdots \mathcal{T}_4$ appear at order $1/m_b^3$. However, these quantities are correlated such that the total number of non-perturbative parameters to order $1/m_b^3$ is the same as in the scheme where m_b is kept finite in the matrix elements which define the non-perturbative parameters. A detailed discussion of these issues can be found in Ref. 43.

In order to define the HQE parameters properly, one must adopt a renormalization scheme, as was done for the heavy quark mass. Since all these parameters can again be determined

by heavy quark sum rules, one may adopt a scheme similar to the kinetic scheme for the quark mass. The HQE parameters in the kinetic scheme depend on powers of the renormalization scale μ , and the above relations are valid in the limit $\mu \rightarrow 0$, leaving only logarithms of μ .

Some of these parameters also appear in the relation for the heavy hadron masses. The quantity $\bar{\Lambda}$ is determined once a definition is specified for the quark mass. The parameter μ_G^2 can be extracted from the mass splitting in the lowest spin-symmetry doublet of heavy mesons

$$\mu_G^2(\mu) = \frac{3}{4}C_G(\mu, m_b)(M_{B^*}^2 - M_B^2), \quad (18)$$

where $C_G(\mu, m_b)$ is a perturbatively-computable coefficient which depends on the scheme. In the kinetic scheme we have

$$\mu_G^2(1\text{GeV}) = 0.35_{-0.02}^{+0.03} \text{ GeV}^2. \quad (19)$$

Determination of HQE Parameters and $|V_{cb}|$

Several experiments have measured moments in $\bar{B} \rightarrow X_c \ell \bar{\nu}_\ell$ decays [44–51] as a function of the minimum lepton momentum. The measurements of the moments of the electron-energy spectrum (0th-3rd), and of the squared-hadronic mass spectrum (0th-2nd), have statistical uncertainties that are roughly equal to their systematic uncertainties. They can be improved with more data and significant effort. Measurements of photon energy moments (0th-2nd) in $B \rightarrow X_s \gamma$ decays [52–55] as a function of the minimum accepted photon energy are still primarily statistics-limited. Global fits to these moments [56–61] have been performed in the 1S and kinetic schemes. A global fit to a large set of hadronic-mass and electron-energy moments in $\bar{B} \rightarrow X_c \ell \bar{\nu}_\ell$ decays in the 1S scheme gives [61]

$$|V_{cb}| = (41.56 \pm 0.39 \pm 0.08) \times 10^{-3} \quad (20)$$

$$m_b^{1\text{S}} = 4.751 \pm 0.058 \text{ GeV} \quad (21)$$

$$\lambda_1^{1\text{S}} = -0.274 \pm 0.047 \text{ GeV}, \quad (22)$$

where the first error includes experimental and theoretical uncertainties, and the second error on $|V_{cb}|$ comes from the B lifetime. The mass value can be compared with a determination

based on the $e^+e^- \rightarrow b\bar{b}$ cross-section near threshold [62] of $m_b^{\text{1S}} = 4.69 \pm 0.03$ GeV. The same data have been fitted in the kinetic scheme, resulting in [58]

$$|V_{cb}| = (41.68 \pm 0.39 \pm 0.58) \times 10^{-3} \quad (23)$$

$$m_b^{\text{kin}} = 4.677 \pm 0.053 \text{ GeV} \quad (24)$$

$$\mu_\pi^2(\text{kin}) = 0.387 \pm 0.039 \text{ GeV} , \quad (25)$$

where the first error includes experimental and theoretical uncertainties, and the second error on $|V_{cb}|$ is from the estimated accuracy of the HQE for the total semileptonic rate. The mass value may be compared with $m_b^{\text{kin}} = 4.56 \pm 0.06$ GeV, extracted from the threshold region of $e^+e^- \rightarrow b\bar{b}$ [63].

In each scheme, theoretical uncertainties are estimated and included in performing the fits. Similar values for the parameters are obtained when only experimental uncertainties are used in the fits, and when photon-energy-spectrum moments from $\bar{B} \rightarrow X_s \gamma$ are included. The χ^2/dof is substantially below unity in all fits, suggesting that the theoretical uncertainties may be overestimated, and showing no evidence for duality violations at a significant level.

The fits in the two schemes agree well on $|V_{cb}|$. We take the arithmetic averages of the values and of the errors to quote an inclusive $|V_{cb}|$ determination:

$$|V_{cb}| = (41.6 \pm 0.6) \times 10^{-3} . \quad (26)$$

The m_b values must be quoted in the same scheme to be directly compared. A translation at NNLO [64] of $m_b^{\text{kin}} = 4.68$ GeV gives

$$m_b^{\text{1S}} = 4.80 \pm 0.01 \text{ GeV} , \quad (27)$$

(the estimated uncertainty comes from varying the scale μ from $m_b/2$ to $2m_b$) to be compared with Eq. (21). The translation of m_b from one scheme to another yields an estimate of the size of the residual uncertainties. While the comparison given above is sensitive to issues beyond scheme translation, the 50 MeV difference serves as an indicator of the size of potential effects. The uncertainties on m_b are further discussed in the section on the determination of $|V_{ub}|$.

The precision of these results can be further improved. The prospects for more precise moments measurements were discussed above. Improvements can be made in the theory by calculating higher-order perturbative corrections [65] and, more importantly, by calculating perturbative corrections to the matrix elements defining the HQE parameters. The inclusion of still-higher-order moments may improve the sensitivity of the fits to higher-order terms in the HQE.

Determination of $|V_{ub}|$

Summary: The determination of $|V_{ub}|$ is the focus of significant experimental and theoretical work. The determinations based on inclusive semileptonic decays using different calculational ansätze are consistent. The total uncertainty is 10%, of which the dominant uncertainty (7%) comes from a 60 MeV error used for m_b . Significant progress has been made in measurements of $\overline{B} \rightarrow \pi \ell \overline{\nu}_\ell$ decays; the branching fraction is now known to 6%, and the q^2 shape is reasonably well constrained experimentally. Further improvements in the form-factor normalization are needed to take full advantage of this precision.

The values obtained from inclusive and exclusive determinations are

$$|V_{ub}| = (4.12 \pm 0.43) \times 10^{-3} \quad (\text{inclusive}), \quad (28)$$

$$|V_{ub}| = (3.5 \begin{smallmatrix} +0.6 \\ -0.5 \end{smallmatrix}) \times 10^{-3} \quad (\text{exclusive}). \quad (29)$$

The two determinations are independent, and the dominant uncertainties are on multiplicative factors. We weight the two values by their relative errors and treat the uncertainties as Gaussian distributed to find

$$|V_{ub}| = (3.95 \pm 0.35) \times 10^{-3}, \quad (30)$$

with $P(\chi^2) = 0.4$.

$|V_{ub}|$ from inclusive decays

The theoretical description of inclusive $\overline{B} \rightarrow X_u \ell \overline{\nu}_\ell$ decays is based on the Heavy Quark Expansion, as for $\overline{B} \rightarrow X_c \ell \overline{\nu}_\ell$ decays, and leads to a predicted total decay rate with uncertainties below 5% [66,67]. Unfortunately, the total decay rate is hard to measure due to the large background from CKM-favored $\overline{B} \rightarrow$

$X_c \ell \bar{\nu}_\ell$ transitions. Calculating the partial decay rate in regions of phase space where $\bar{B} \rightarrow X_c \ell \bar{\nu}_\ell$ decays are suppressed is more challenging, as the HQE convergence in these regions is spoiled, requiring the introduction of a non-perturbative distribution function, the “shape function” (SF) [68,69], whose form is unknown. The shape function becomes important when the light-cone momentum component $P_+ \equiv E_X - |P_X|$ is not large compared to Λ_{QCD} . This additional difficulty can be addressed in two complementary ways. The leading-shape function can either be measured in the radiative decay $\bar{B} \rightarrow X_s \gamma$, or be modeled with constraints on the 0th-2nd moments, and the results applied to the calculation of the $\bar{B} \rightarrow X_u \ell \bar{\nu}_\ell$ partial decay rate [70–72]; in such an approach, the largest challenges are for the theory. Alternatively, measurements of $\bar{B} \rightarrow X_u \ell \bar{\nu}_\ell$ partial decay rates can be extended further into the $\bar{B} \rightarrow X_c \ell \bar{\nu}_\ell$ -allowed region, enabling a simplified theoretical (pure HQE) treatment [73], but requiring precise experimental knowledge of the $\bar{B} \rightarrow X_c \ell \bar{\nu}_\ell$ background.

The shape function is a universal property of B mesons at leading order. It has been recognized for over a decade [68,69] that the leading SF can be measured in $\bar{B} \rightarrow X_s \gamma$ decays. However, sub-leading shape functions [74–79] arise at each order in $1/m_b$, and differ in semileptonic and radiative B decays. The form of the shape functions cannot be calculated from first principles. Prescriptions that relate directly the partial rates for $\bar{B} \rightarrow X_s \gamma$ and $\bar{B} \rightarrow X_u \ell \bar{\nu}_\ell$ decays, and thereby avoid any parameterization of the leading shape function, are available [80–83]; uncertainties due to sub-leading SF remain in these approaches. Existing measurements, however, have tended to use parameterizations of the leading SF that respect constraints on the zeroth, first, and second moments. At leading order, the first and second moments are equal to $\bar{\Lambda} = M_B - m_b$ and μ_π^2 , respectively. The relations between SF moments and the non-perturbative parameters of the HQE are known to second order in α_s [84]. As a result, measurements of HQE parameters from global fits to $\bar{B} \rightarrow X_c \ell \bar{\nu}_\ell$ and $\bar{B} \rightarrow X_s \gamma$ moments can be used to constrain the SF moments, as well as provide accurate values of m_b and other parameters for use

in determining $|V_{ub}|$. The possibility of measuring these HQE parameters directly from moments in $\bar{B} \rightarrow X_u \ell \bar{\nu}_\ell$ decays has been explored [85], but the experimental precision achievable there is not competitive with other approaches.

The calculations which are used for the fits performed by HFAG are documented in Refs. [70](BLNP), [86](GGOU), [87](DGE), and [73](BLL).

The calculations start from the triple differential rate using the variables

$$P_l = M_B - 2E_l, \quad P_- = E_X + |\vec{P}_X|, \quad P_+ = E_X - |\vec{P}_X| \quad (31)$$

for which the differential rate becomes

$$\begin{aligned} \frac{d^3\Gamma}{dP_+ dP_- dP_l} &= \frac{G_F^2 |V_{ub}|^2}{16\pi^2} (M_B - P_+) \quad (32) \\ &\left\{ (P_- - P_l)(M_B - P_- + P_l - P_+) \mathcal{F}_1 \right. \\ &\left. + (M_B - P_-)(P_- - P_+) \mathcal{F}_2 + (P_- - P_l)(P_l - P_+) \mathcal{F}_3 \right\}. \end{aligned}$$

The “structure functions” \mathcal{F}_i can be calculated using factorization theorems that have been proven to subleading order in the $1/m_b$ expansion.

The BLNP [70] calculation uses these factorization theorems to write the \mathcal{F}_i in terms of perturbatively-calculable hard coefficients H and jet functions J , which are convolved with the (soft) light-cone distribution functions S , the shape functions of the B meson.

The leading order term in the $1/m_b$ expansion of the \mathcal{F}_i contains a single non-perturbative function, and is calculated to subleading order in α_s , while at subleading order in the $1/m_b$ expansion, there are several independent non-perturbative functions which have been calculated only at tree level in the α_s expansion.

To extract the non-perturbative input, one can study the photon-energy spectrum in $B \rightarrow X_s \gamma$ [72]. This spectrum is known at a similar accuracy as the P_+ spectrum in $B \rightarrow X_u \ell \bar{\nu}_\ell$. Going to subleading order in the $1/m_b$ expansion requires the modeling of subleading SFs, a large variety of which were studied in Ref. 70.

A recent calculation (GGOU) [86] uses a hard, Wilsonian cut-off that matches the definition of the kinetic mass. The non-perturbative input is similar to what is used in BLNP, but the shape functions are defined differently. In particular, they are defined at finite m_b , and depend on the light-cone component k_+ of the b quark momentum, and on the momentum transfer q^2 to the leptons. These functions include sub-leading effects to all orders; as a result, they are non-universal, with one shape function corresponding to each structure function in Eq. (32). Their k_+ moments can be computed in the OPE, and related to observables and to the shape functions defined in Ref. 70.

Going to subleading order in α_s requires the definition of a renormalization scheme for the HQE parameters and for the shape function. It has been noted that the relation between the moments of the shape function and the forward matrix elements of local operators is plagued by ultraviolet problems which require additional renormalization. A possible scheme for improving this behavior has been suggested in Refs. [70,72], which introduce a particular definition of the quark mass (the so-called shape-function scheme) based on the first moment of the measured spectrum. Likewise, the HQE parameters can be defined from measured moments of spectra, corresponding to moments of the shape function.

One can also attempt to calculate the SF by using additional assumptions. One possible approach (DGE) is the so-called “dressed gluon approximation” [87], where the perturbative result is continued into the infrared regime using the renormalon structure obtained in the large β_0 limit, where β_0 has been defined following Eq. (16). Alternatively, one may assume an analytic behaviour for the strong coupling in the infrared to perform an extrapolation of perturbation theory [88].

While attempts to quantify the shape function are important, the impact of uncertainties in the shape function is significantly reduced in some recent measurements that cover a larger portion of the $\bar{B} \rightarrow X_u \ell \bar{\nu}_\ell$ phase space. Several measurements using a combination of cuts on the leptonic momentum transfer q^2 and the hadronic invariant mass M_X , as suggested

in Ref. 89, have been made. Measurements of the electron spectrum in $\overline{B} \rightarrow X_u \ell \overline{\nu}_\ell$ decays have been made down to 1.9 GeV, at which point shape-function uncertainties are not dominant. The measurements quoted below have used a variety of functional forms to parameterize the leading shape function; in no case does this lead to more than a 2% uncertainty on $|V_{ub}|$.

Weak Annihilation [86,90,91](WA) can in principle contribute significantly in the restricted region (at high q^2) accepted by measurements of $\overline{B} \rightarrow X_u \ell \overline{\nu}_\ell$ decays. An estimate [73] based on leptonic D_s decays [91] leads to a $\sim 3\%$ uncertainty on the total $\overline{B} \rightarrow X_u \ell \overline{\nu}_\ell$ rate from the $\Upsilon(4S)$. The differential spectrum from WA decays is not known, but they are expected to contribute predominantly at high q^2 , and may be a significant source of uncertainty for $|V_{ub}|$ measurements that only accept a small fraction, f_u , of the full $\overline{B} \rightarrow X_u \ell \overline{\nu}_\ell$ phase space. Model-dependent limits on WA were determined in Ref. 92, where the CLEO data were fitted to combinations of WA models and a spectator $\overline{B} \rightarrow X_u \ell \overline{\nu}_\ell$ component and background. More direct experimental constraints [93] on WA have recently been made by comparing the $\overline{B} \rightarrow X_u \ell \overline{\nu}_\ell$ decay rates of charged and neutral B mesons. The sensitivity of $|V_{ub}|$ determinations to WA can also be reduced by removing the region at high q^2 in those measurements where q^2 is determined.

Measurements

We summarize the measurements used in the determination of $|V_{ub}|$ below. Given the improved precision and more rigorous theoretical interpretation of the recent measurements, earlier determinations [94–97] will not be further considered in this review.

Electron momentum “endpoint” measurements [98–100] reconstruct a single charged electron to determine a partial decay rate for $\overline{B} \rightarrow X_u \ell \overline{\nu}_\ell$. This results in a high $\mathcal{O}(50\%)$ selection efficiency and only modest sensitivity to the modeling of detector response. The decay rate can be cleanly extracted for $E_e > 2.3$ GeV, but this is deep in the SF region, where theoretical uncertainties are large. Measurements down to 2.0 or 1.9 GeV exist, but have low ($< 1/10$) signal-to-background (S/B) ratio, making the control of the $\overline{B} \rightarrow X_c \ell \overline{\nu}_\ell$ background

a crucial point. In these analyses, the inclusive electron momentum spectrum from $B\bar{B}$ events is determined by subtracting the $e^+e^- \rightarrow q\bar{q}$ continuum background using data samples collected just below $B\bar{B}$ threshold. The continuum-subtracted spectrum is fitted to a combination of a model $\bar{B} \rightarrow X_u\ell\bar{\nu}_\ell$ spectrum and several components ($D\ell\bar{\nu}_\ell$, $D^*\ell\bar{\nu}_\ell$, ...) of the $\bar{B} \rightarrow X_c\ell\bar{\nu}_\ell$ background. The resulting partial branching fractions for various E_e cuts are given in Table 1. The leading uncertainty at the lower lepton momentum cuts comes from the $\bar{B} \rightarrow X_c\ell\bar{\nu}_\ell$ background. Prospects for further reducing the lepton momentum cut are improving in light of better knowledge of the semileptonic decays to higher mass $X_c\ell\bar{\nu}$ states [22,23]. The determination of $|V_{ub}|$ from these measurements is discussed below.

An untagged “neutrino reconstruction” measurement [101] from BaBar uses a combination [102] of a high-energy electron, with a measurement of the missing momentum vector. This allows a much higher S/B ~ 0.7 at the same E_e cut and a $\mathcal{O}(5\%)$ selection efficiency, but at the cost of a smaller accepted phase space for $\bar{B} \rightarrow X_u\ell\bar{\nu}_\ell$ decays and uncertainties associated with the determination of the missing momentum. A control sample of $\Upsilon(4S) \rightarrow B\bar{B}$ decays where one B is reconstructed as $\bar{B} \rightarrow D^0(X)e\bar{\nu}$ with $D^0 \rightarrow K^-\pi^+$ is used to reduce uncertainties from detector and background modeling. The partial branching fraction and $|V_{ub}|$ are given in Table 1.

The large samples accumulated at the B factories allow studies in which one B meson is fully reconstructed and the recoiling B decays semileptonically [103–105]. The experiments can fully reconstruct a “tag” B candidate in about 0.5% (0.3%) of B^+B^- ($B^0\bar{B}^0$) events. An electron or muon with center-of-mass momentum above 1.0 GeV is required amongst the charged tracks not assigned to the tag B , and the remaining particles are assigned to the X_u system. The full set of kinematic properties (E_ℓ , M_X , q^2 , etc.) are available for studying the semileptonically decaying B , making possible selections that accept up to 70% of the full $\bar{B} \rightarrow X_u\ell\bar{\nu}_\ell$ rate. Despite requirements (*e.g.*, on the square of the missing mass) aimed at rejecting events with

additional missing particles, undetected or mis-measured particles from $\overline{B} \rightarrow X_c \ell \overline{\nu}_\ell$ decay (*e.g.*, K_L^0 and additional neutrinos) remain an important source of uncertainty.

BaBar [103] and Belle [104] have measured partial rates with cuts on M_X , M_X , and q^2 , and P_+ based on large samples of $B\overline{B}$ events. As these are highly correlated measurements, only one from each experiment (namely based on M_X) is used in the average given in Table 1. In each case, the experimental systematics have significant contributions from the modeling of $\overline{B} \rightarrow X_u \ell \overline{\nu}_\ell$ and $\overline{B} \rightarrow X_c \ell \overline{\nu}_\ell$ decays, and from the detector response to charged particles, photons, and neutral hadrons.

An analysis [105] on 80 fb^{-1} that integrates the $\overline{B} \rightarrow X_u \ell \overline{\nu}_\ell$ rate for $M_X < 2.5 \text{ GeV}$, capturing $\sim 96\%$ of the total rate, is noteworthy for the smallness ($< 3\%$) of the theoretical error; however, the statistical uncertainty on $|V_{ub}|$ is 18%, so it would have no impact if included in the current average. More precise measurements of this type would be valuable.

Determination of $|V_{ub}|$

The determination of $|V_{ub}|$ from the measured partial rates requires input from theory. The BLNP, GGOU, and DGE calculations described previously are used to determine $|V_{ub}|$ from all measured partial $\overline{B} \rightarrow X_u \ell \overline{\nu}_\ell$ rates; the values are given in Table 1. The m_b input values used [106] are $m_b^{SF} = 4.71 \pm 0.06 \text{ GeV}$ for BLNP, based on global fits to $\overline{B} \rightarrow X_c \ell \overline{\nu}_\ell$ moments; $m_b^{\text{kin}} = 4.61 \pm 0.03 \text{ GeV}$ for GGOU, based on global fits to $\overline{B} \rightarrow X_c \ell \overline{\nu}_\ell$ and $\overline{B} \rightarrow X_s \gamma$ moments; and $m_b^{\overline{MS}} = 4.20 \pm 0.07 \text{ GeV}$ for DGE, based on an average of m_b determinations. While these values are compatible within errors, they do not correspond to a unique value when translated to a common scheme; this is further discussed below. An additional error contribution for WA has been added to the DGE error budget.

As an illustration of the relative sizes of the uncertainties entering $|V_{ub}|$, we give the error breakdown for the BLNP average: statistical—2.0%; experimental—2.5%; $\overline{B} \rightarrow X_c \ell \overline{\nu}_\ell$ modeling—1.8%; $\overline{B} \rightarrow X_u \ell \overline{\nu}_\ell$ modeling—1.1%; HQE parameters (including m_b)—6.3%; shape-function parameterization—0.4%; subleading SFs—0.7%; scale matching—3.6%; Weak Annihilation—1.4%.

The uncertainty on m_b dominates the uncertainty on $|V_{ub}|$ from HQE parameters.

Table 1: $|V_{ub}|$ (in units of 10^{-5}) from inclusive $\overline{B} \rightarrow X_u \ell \overline{\nu}_\ell$ measurements. The first uncertainty on $|V_{ub}|$ is experimental, while the second includes both theoretical ($\sim 4\%$) and HQE parameter uncertainties (the remainder). The values are listed in order of increasing f_u (0.19 to 0.66).

Ref.	BLNP	GGOU	DGE
[98]	$353 \pm 41 \pm 35$	$371 \pm 43 \pm 32$	$386 \pm 45 \pm 28$
[101]	$395 \pm 27 \pm 39$	not avail.	$443 \pm 30 \pm 37$
[100]	$390 \pm 22 \pm 33$	$408 \pm 23 \pm 27$	$430 \pm 29 \pm 25$
[99]	$437 \pm 40 \pm 33$	$456 \pm 42 \pm 26$	$481 \pm 45 \pm 22$
[107]	$398 \pm 42 \pm 32$	$416 \pm 44 \pm 29$	$444 \pm 47 \pm 22$
[103]	$374 \pm 18 \pm 31$	$402 \pm 19 \pm 28$	$456 \pm 22 \pm 30$
[104]	$366 \pm 24 \pm 27$	$389 \pm 26 \pm 22$	$429 \pm 28 \pm 26$
	$399 \pm 14 \pm 30$	$395 \pm 15 \pm 21$	$443 \pm 17 \pm 25$

The statistical correlations amongst the measurements used in the average are tiny (due to small overlaps among signal events and large differences in S/B ratios), and have been ignored in performing the average. Correlated systematic and theoretical errors are taken into account, both within an experiment and between experiments.

The $|V_{ub}|$ values do not show a marked trend versus f_u . The P-values of the averages are around 0.4, suggesting that the ratios of calculated partial widths in the different phase space regions are in reasonable agreement with ratios of measured widths. However, the measured values [103,104] of the ratio $\Gamma(\overline{B} \rightarrow X_u \ell \overline{\nu}_\ell, P_+ < 0.66 \text{ GeV}) / \Gamma(\overline{B} \rightarrow X_u \ell \overline{\nu}_\ell, M_X < 1.7 \text{ GeV}, q^2 > 8 \text{ GeV}^2)$ average[†] to 1.22 ± 0.12 . The theoretical predictions for this ratio are 1.63 [70], 1.18 [86], and

[†] This assumes that the correlation coefficient between the P_+ and M_X - q^2 partial branching fractions found by BaBar, 0.38, also applies to the Belle measurements.

1.58 [87]. This comparison may indicate an underestimate of some theoretical uncertainties.

The BLNP and GGOU averages appear to agree well. However, if the same m_b input is used for BLNP and GGOU, the BLNP average is $\sim 9\%$ higher than the GGOU average. This difference is large compared to the theoretical uncertainties assigned to the calculations, which are 3-4% in each case. Based on this comparison, we choose to add in quadrature an additional uncertainty of 7% to the inclusive $|V_{ub}|$ average.

To quote an inclusive $|V_{ub}|$ value, we take the arithmetic mean of the values in Table 1. The uncertainty is calculated by summing in quadrature the arithmetic mean of the errors in Table 1 (after adjusting them to correspond to $\sigma_{m_b} = 0.06$ GeV), and the aforementioned 7% additional uncertainty. We find

$$|V_{ub}| = (4.12 \pm 0.15_{\text{exp}} \pm 0.40_{\text{th}}) \times 10^{-3} . \quad (33)$$

As was the case with $|V_{cb}|$, it is hard to assign an uncertainty to $|V_{ub}|$ for possible duality violations. However, theoretical arguments suggest that duality should hold even better in $b \rightarrow u\ell\bar{\nu}_\ell$ than in $b \rightarrow c\ell\bar{\nu}_\ell$ [32]. On the other hand, unless duality violations are much larger in $\bar{B} \rightarrow X_u\ell\bar{\nu}_\ell$ decays than in $\bar{B} \rightarrow X_c\ell\bar{\nu}_\ell$ decays, the precision of the $|V_{ub}|$ determination is not yet at the level where duality violations are likely to be significant.

There is another aspect of duality which affects the quoted results. The theoretical expressions are valid at the parton level, and do not incorporate any resonant structure (*e.g.* $\bar{B} \rightarrow \pi\ell\bar{\nu}_\ell$); this must be added “by hand” to the simulated $\bar{B} \rightarrow X_u\ell\bar{\nu}_\ell$ event samples used to calculate acceptances and efficiencies. The uncertainties corresponding to this procedure have been estimated by the experiments to be at the level of 1-2% on $|V_{ub}|$.

A separate class of analyses follows the strategy discussed in Refs. [80–83], where integrals of differential distributions in $\bar{B} \rightarrow X_u\ell\bar{\nu}_\ell$ decays are compared with corresponding integrals in $\bar{B} \rightarrow X_s\gamma$ decays to extract $|V_{ub}|$, thereby eliminating the need to model the leading-shape function. A study [108] using

the measured BaBar electron spectrum in $\overline{B} \rightarrow X_u \ell \overline{\nu}_\ell$ decays provides $|V_{ub}|$ determinations using all available “SF-free” calculations; the resulting $|V_{ub}|$ values have total uncertainties of $\sim 12\%$, and are fully compatible with the average quoted above.

The BLL [89] calculation can be used for measurements with cuts on M_X and q^2 . Using the HQE parameter input determined from the global fit in the 1S scheme [61] yields a $|V_{ub}|$ value of $(4.83 \pm 0.24 \pm 0.37) \times 10^{-3}$, which is 7 – 17% higher than the corresponding values obtained from the other calculations.

HQE parameters and shape function input

The global fits to $\overline{B} \rightarrow X_c \ell \overline{\nu}_\ell$ moments discussed earlier provide input values for the heavy quark parameters needed in calculating $\overline{B} \rightarrow X_u \ell \overline{\nu}_\ell$ partial rates. These HQE parameters are also used to constrain the first and second moments of the shape function.

Fig. 2 shows the results of separate fits to moments from semileptonic decays, and those from the $\overline{B} \rightarrow X_s \gamma$ photon energy spectrum. The ellipses correspond to $\Delta\chi^2 = 1$ contours (CL=39%); the probability of having the two ellipses separated by as much or more than the fit results is about 20%. The $\overline{B} \rightarrow X_s \gamma$ moments have some dependence [109] on the model chosen for the shape function, since the experiments require photon energies to exceed cuts in the range 1.8-2.0 GeV. The global fit assumes an uncertainty of 30% on the difference between the calculated moments with a realistic shape function model and those based on the pure OPE calculation.

The uncertainty on m_b will continue to be a leading contribution to the uncertainty in $|V_{ub}|$. The determinations of m_b using $\overline{B} \rightarrow X_c \ell \overline{\nu}_\ell$ moments are on solid theoretical ground and are performed using order α_S^2 calculations. Concern has been expressed about the theoretical control of $\mathcal{O}(1/m_b)$ corrections to the $\overline{B} \rightarrow X_s \gamma$ moments. Furthermore, the $|V_{ub}|$ calculations are currently done at $\mathcal{O}(\alpha_S)$, calling into question the use of a very small uncertainty on m_b in the $|V_{ub}|$ determination. Fixed-order translations of m_b from one scheme to another bring in an additional source of uncertainty (see Eq. (27)). In light of

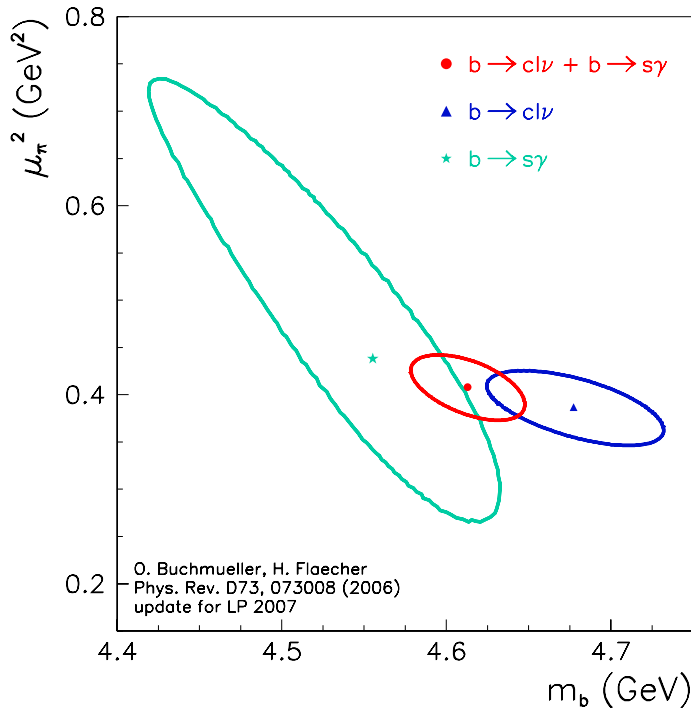


Figure 2: Fit results from global moment fits in the kinetic scheme [58]. The $\Delta\chi^2 = 1$ curves for separate fits to $\overline{B} \rightarrow X_s \gamma$ moments and $\overline{B} \rightarrow X_c \ell \bar{\nu}_\ell$ moments are shown along with the combined fit.

these considerations, the m_b used in the $|V_{ub}|$ determination given here has had its error increased to 0.06 GeV.

Status and outlook

At present, as indicated by the average given above, the uncertainty on $|V_{ub}|$ from inclusive decays is at the 10% level. The uncertainty on m_b taken here is 60 MeV, contributing an uncertainty of 7% on $|V_{ub}|$. Prospects are good for reducing this to the 30 MeV level by extending the $|V_{ub}|$ calculations to $\mathcal{O}(\alpha_S^2)$. Further progress can also be expected on some of the other leading sources of uncertainty. The Weak Annihilation contribution is now being addressed with data; further improvement can be expected with the full B factory dataset.

The uncertainties on $|V_{ub}|$ quoted in the calculations are at the 4% level, and there is some indication that these may be underestimated. Improving our confidence in, and eventually reducing, these theory uncertainties will require improvements in the calculations. For the approaches making use of the shape function, this amounts to improvements in relating the spectra from $\overline{B} \rightarrow X_u \ell \overline{\nu}_\ell$ and $\overline{B} \rightarrow X_s \gamma$ decays by calculating radiative corrections and the effects of subleading shape functions, while approaches less sensitive to shape functions require calculations of higher-order radiative corrections. Experimental uncertainties will be reduced through higher statistics, a better understanding of $\overline{B} \rightarrow X_c \ell \overline{\nu}_\ell$ decays, and the incorporation of improved measurements on D decays. The two approaches stated earlier, namely determining the shape function from the $\overline{B} \rightarrow X_s \gamma$ photon spectrum, and applying it to $\overline{B} \rightarrow X_u \ell \overline{\nu}_\ell$ decays, and pushing the measurements into regions where shape function and duality uncertainties become negligible, are complementary and should both be pursued.

$|V_{ub}|$ from exclusive decays

Exclusive charmless semileptonic decays offer a complementary means of determining $|V_{ub}|$. For the experiments, the specification of the final state provides better background rejection, but the lower branching fraction reflects itself in lower yields compared with inclusive decays. For theory, the calculation of the form factors for $\overline{B} \rightarrow X_u \ell \overline{\nu}_\ell$ decays is challenging, but brings in a different set of uncertainties from those encountered in inclusive decays. In this review, we focus on $\overline{B} \rightarrow \pi \ell \overline{\nu}_\ell$, as it is the most promising mode for both experiment and theory, and recent improvements have been made in both areas. Measurements of other exclusive states can be found in Refs. [110–113].

$\overline{B} \rightarrow \pi \ell \overline{\nu}_\ell$ form factor calculations

The relevant form factors for the decay $\overline{B} \rightarrow \pi \ell \overline{\nu}_\ell$ are usually defined as

$$\begin{aligned} \langle \pi(p_\pi) | V^\mu | B(p_B) \rangle = & \quad (34) \\ f_+(q^2) \left[p_B^\mu + p_\pi^\mu - \frac{m_B^2 - m_\pi^2}{q^2} q^\mu \right] + f_0(q^2) \frac{m_B^2 - m_\pi^2}{q^2} q^\mu, \end{aligned}$$

in terms of which the rate becomes (in the limit $m_\ell \rightarrow 0$)

$$\frac{d\Gamma}{dq^2} = \frac{G_F^2 |V_{ub}|^2}{24\pi^3} |p_\pi|^3 |f_+(q^2)|^2, \quad (35)$$

where p_π is the momentum of pion in the B meson rest frame.

Currently-available non-perturbative methods for the calculation of the form factors include lattice QCD and light-cone sum rules. The two methods are complementary in phase space, since the lattice calculation is restricted to the kinematical range of high momentum transfer q^2 to the leptons, due to large discretization errors, while light-cone sum rules provide information near $q^2 = 0$. Interpolations between these two regions may be constrained by unitarity and analyticity.

Unquenched simulations, for which quark loop effects in the QCD vacuum are fully incorporated, have become quite common, and the first results based on these simulations for the $\overline{B} \rightarrow \pi \ell \overline{\nu}_\ell$ form factors have been obtained recently by the Fermilab/MILC collaboration [25] and the HPQCD collaboration [114].

The two calculations differ in the way the b quark is simulated, with HPQCD using nonrelativistic QCD, and Fermilab/MILC the so-called Fermilab heavy quark method; they agree within the quoted errors.

In order to obtain the partially-integrated differential rate, the BK parameterization [115]

$$f_+(q^2) = \frac{c_B(1 - \alpha_B)}{(1 - \tilde{q}^2)(1 - \alpha_B \tilde{q}^2)}, \quad (36)$$

$$f_0(q^2) = \frac{c_B(1 - \alpha_B)}{(1 - \tilde{q}^2/\beta_B)}, \quad (37)$$

with $\tilde{q}^2 \equiv q^2/m_{B^*}^2$ is used to extrapolate to small values of q^2 . It includes the leading pole contribution from B^* , and higher poles are modeled by a single pole. The heavy-quark scaling is satisfied if the parameters c_B , α_B , and β_B scale appropriately. However, the BK parameterization should be used with some caution, since it is not consistent with SCET [116]. Alternatively, one may use analyticity and unitarity bounds to constrain the form factors. Making use of the heavy quark limit, stringent constraints on the shape of the form factor can be

derived [117], and the conformal mapping of the kinematical variables onto the complex unit disc yields a rapidly converging series in this variable. The use of lattice data in combination with a data point at small q^2 from SCET or sum rules provides a stringent constraint on the shape of the form factor [118].

The results for the integrated rate with $q^2 > q_{\text{cut}}^2 = 16\text{GeV}^2$ are

$$\begin{aligned}\Gamma &= |V_{ub}|^2 \times (2.07 \pm 0.57) \text{ps}^{-1}, & \text{HPQCD;} \\ &= |V_{ub}|^2 \times (1.83 \pm 0.50) \text{ps}^{-1}, & \text{Fermilab/MILC.}\end{aligned}$$

Here the statistical and systematic errors are added in quadrature.

Much work remains to be done, since the current combined statistical plus systematic errors in the lattice results are still at the 10-14% level on $|V_{ub}|$, and need to be reduced. Reduction of errors to the 5 ~ 6% level for $|V_{ub}|$ may be feasible within the next few years, although that could involve carrying out a two-loop (or fully non-perturbative) matching between lattice and continuum QCD heavy-to-light current operators, and/or going to smaller lattice spacing.

Another established non-perturbative approach to obtain the form factors is through Light-Cone QCD Sum Rules (LCSR), where the heavy mass limit has been discussed from the point of view of SCET in [119]. The sum-rule approach provides an approximation for the product $f_B f_+(q^2)$, valid in the region $0 < q^2 < \sim 14 \text{GeV}^2$. The determination of $f_+(q^2)$ itself requires knowledge of the decay constant f_B , which usually is obtained by replacing f_B by its two-point QCD (SVZ) sum rule [120] in terms of perturbative and condensate contributions. The advantage of this procedure is the approximate cancellation of various theoretical uncertainties in the ratio $(f_B f_+)/f_B$. The LCSR for $f_B f_+$ is based on the light-cone OPE of the relevant vacuum-to-pion correlation function, calculated in full QCD at finite b -quark mass. The resulting expressions actually comprise a triple expansion: in the twist t of the operators near the light-cone, in α_s , and in the deviation of the pion distribution amplitudes from their asymptotic form, which is fixed from conformal symmetry.

There are multiple sources of uncertainties in the LCQCD calculation, which are discussed in Refs. [121,122]. The total uncertainty adds up to about 15%, resulting in the LCQCD prediction

$$f_+(0) = 0.26 \pm 0.04 , \quad (38)$$

which is consistent with the values quoted in Refs. [121] and [122]. It is interesting to note that the results from the LQCD and LCSR are consistent with each other when the BK parameterization is used to relate them. This increases confidence in the theoretical predictions for the rate of $\overline{B} \rightarrow \pi \ell \overline{\nu}_\ell$.

LC-sum rules are valid in the kinematic region of small q^2 , and thus can be used to obtain an estimate of the q^2 dependence in a region $q^2 \leq 14\text{GeV}^2$ [123]. This is complementary to the lattice results at large values of q^2 , and the results from LCQCD smoothly extrapolate the lattice data to small values of q^2 .

An alternative determination of $|V_{ub}|$ has been proposed by several authors [124–125]. It is based on a model-independent relation between rare decays such as $\overline{B} \rightarrow K^* \ell^+ \ell^-$ and $\overline{B} \rightarrow \rho \ell \overline{\nu}_\ell$, which can be obtained at large momentum transfer q to the leptons. This method is based on the HQET relations between the matrix elements of the $B \rightarrow K^*$ and the $B \rightarrow \rho$ transitions, and a systematic, OPE-based expansion in powers of m_c^2/q^2 and Λ_{QCD}/q . The theoretical uncertainty is claimed to be of the order of 5% for $|V_{ub}|$; however, it requires a precise measurement of the exclusive rare decay $\overline{B} \rightarrow K^* \ell^+ \ell^-$, which is a task for future ultra-high-rate experiments.

$\overline{B} \rightarrow \pi \ell \overline{\nu}_\ell$ measurements

The $\overline{B} \rightarrow \pi \ell \overline{\nu}_\ell$ measurements fall into two broad classes: untagged, in which case the reconstruction of the missing momentum of the event serves as an estimator for the unseen neutrino, and tagged, in which the second B meson in the event is fully reconstructed in either a hadronic or semileptonic decay mode. The tagged measurements have high and uniform acceptance, S/B as high as 10, but low statistics. The untagged measurements have somewhat higher background levels (S/B \leq 1) and make slightly more restrictive kinematic cuts, but have adequate statistics to measure the q^2 dependence of the form factor.

Table 2: Total and partial branching fractions for $\overline{B}^0 \rightarrow \pi^+ \ell^- \overline{\nu}_\ell$. The uncertainties are from statistics and systematics. Measurements of $\mathcal{B}(B^- \rightarrow \pi^0 \ell^- \overline{\nu}_\ell)$ have been multiplied by a factor $2\tau_{B^0}/\tau_{B^+}$ to obtain the values below.

	$\mathcal{B} \times 10^4$	$\mathcal{B}(q^2 > 16) \times 10^4$
CLEO π^+, π^0 [112]	$1.37 \pm 0.15 \pm 0.11$	$0.41 \pm 0.08 \pm 0.04$
BaBar π^+, π^0 [126]	$1.46 \pm 0.07 \pm 0.08$	$0.38 \pm 0.04 \pm 0.03$
Belle SL π^+ [127]	$1.38 \pm 0.19 \pm 0.14$	$0.36 \pm 0.10 \pm 0.04$
Belle SL π^0 [127]	$1.43 \pm 0.26 \pm 0.16$	$0.37 \pm 0.15 \pm 0.04$
Belle had π^+ [128]	$1.49 \pm 0.26 \pm 0.06$	NA
Belle had π^0 [128]	$1.60 \pm 0.32 \pm 0.11$	NA
BaBar SL π^+ [129]	$1.12 \pm 0.25 \pm 0.10$	$0.29 \pm 0.15 \pm 0.04$
BaBar SL π^0 [129]	$1.36 \pm 0.33 \pm 0.15$	$0.19 \pm 0.22 \pm 0.07$
BaBar had π^+ [129]	$1.07 \pm 0.27 \pm 0.15$	$0.65 \pm 0.20 \pm 0.13$
BaBar had π^0 [129]	$1.52 \pm 0.41 \pm 0.20$	$0.48 \pm 0.22 \pm 0.11$
Average	$1.39 \pm 0.06 \pm 0.06$	$0.35 \pm 0.03 \pm 0.03$

CLEO has analyzed $\overline{B} \rightarrow \pi \ell \overline{\nu}_\ell$ and $\overline{B} \rightarrow \rho \ell \overline{\nu}_\ell$ using an untagged analysis [112]. Similar analyses have been done by BaBar [113,126]. The leading systematic uncertainties in the untagged $\overline{B} \rightarrow \pi \ell \overline{\nu}_\ell$ analyses are associated with modeling the missing momentum reconstruction, with backgrounds from $\overline{B} \rightarrow X_c \ell \overline{\nu}_\ell$ and $\overline{B} \rightarrow X_u \ell \overline{\nu}_\ell$ decays, and with varying the form factor for the $\overline{B} \rightarrow \rho \ell \overline{\nu}_\ell$ decay. The values obtained for the full and partial branching fractions are listed in Table 2 above the horizontal line.

BaBar has recently measured the differential $\overline{B} \rightarrow \pi \ell \overline{\nu}_\ell$ rate versus q^2 with good accuracy [126]. A fit using the BK parameterization [115] gives $\alpha = 0.52 \pm 0.05 \pm 0.03$ with $P(\chi^2) = 65\%$. The q^2 spectrum, shown in Fig. 3, is compatible with the shapes expected from both LCSR and LQCD calculations, but is incompatible ($P(\chi^2) = 0.06\%$) with the ISGW2 [130] model.

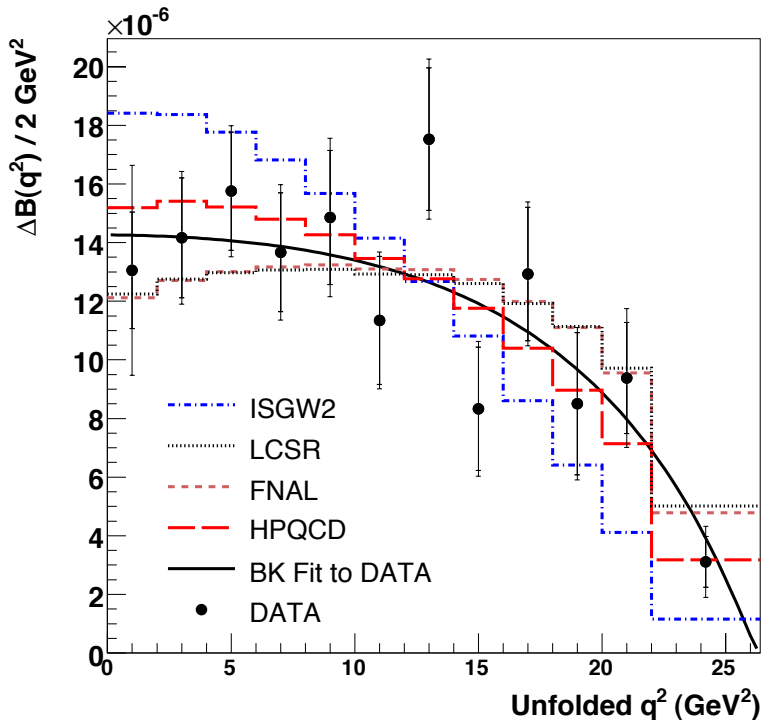


Figure 3: The differential branching fraction versus q^2 from BaBar [126] with several theoretical predictions overlaid.

Belle [127] and BaBar [129] have performed analyses based on reconstructing a B in the $\overline{D}^{(*)}\ell^+\nu_\ell$ decay mode, and looking for a $\overline{B} \rightarrow \pi\ell\overline{\nu}_\ell$ or $\overline{B} \rightarrow \rho\ell\overline{\nu}_\ell$ decay amongst the remaining particles in the event. The fact that the B and \overline{B} are back-to-back in the $\Upsilon(4S)$ frame is used to construct a discriminating variable and obtain a signal-to-noise ratio above unity for all q^2 bins. A related technique was discussed in Ref. 131. BaBar [129] and Belle [128] have also used their samples of B mesons reconstructed in hadronic decay modes to measure exclusive charmless semileptonic decays giving very clean but low-yield samples. The resulting full and partial branching fractions are given in Table 2. The average of the tagged analyses provides an accuracy on the $\overline{B} \rightarrow \pi\ell\overline{\nu}_\ell$ branching fraction comparable to that obtained with untagged analyses.

The outlook for further improvements in these measurements with larger B-factory data samples is good. The tagged measurements in particular will improve; the current estimates of systematic uncertainties in these measurements have a significant statistical component, so the total experimental uncertainty should fall as $1/\sqrt{N}$.

$|V_{ub}|$ can be obtained from the average $\overline{B} \rightarrow \pi \ell \overline{\nu}_\ell$ branching fraction and the measured q^2 spectrum. Fits to the measured q^2 spectrum from Ref. 126 using a theoretically motivated parameterization (*e.g.*, from Ref. 9) remove most of the model dependence from theoretical uncertainties in the shape of the spectrum. This allows a good determination [132] of the product

$$|V_{ub}|f_+(0) = (9.1 \pm 0.3 \pm 0.6) \times 10^{-4}, \quad (39)$$

where the first error is from the uncertainty on $\mathcal{B}(\overline{B} \rightarrow \pi \ell \overline{\nu}_\ell)$, and the second from the parameterization of shape versus q^2 . Having the shape of the form factor versus q^2 allows determinations of the normalization at any q^2 value to be used. Several determinations of $|V_{ub}|$ are given in Table 3, where the LQCD results have been expressed as $f_+(0)$ using the aforementioned fit to the measured q^2 spectrum. Based on these values we pick

$$|V_{ub}| = (3.5^{+0.6}_{-0.5}) \times 10^{-3}. \quad (40)$$

The uncertainty is dominated by the form factor normalization, the calculations of which were discussed previously.

Table 3: Determinations of $|V_{ub}|$ based on $\overline{B} \rightarrow \pi \ell \overline{\nu}_\ell$ decays. The first error on $|V_{ub}|$ is due to the uncertainty on $|V_{ub}|f_+(0)$ and the second error comes from uncertainty on $f_+(0)$.

Method	$f_+(0)$	$ V_{ub} \times (10^{-3})$
LCSR (Eq. (38))	0.26 ± 0.04	$3.5 \pm 0.3^{+0.6}_{-0.5}$
LQCD(FNAL) [25]	0.25 ± 0.03	$3.6 \pm 0.3^{+0.5}_{-0.4}$
LQCD(HPQCD) [114]	0.27 ± 0.03	$3.3 \pm 0.3^{+0.4}_{-0.3}$

Conclusion

The study of semileptonic B meson decays continues to be an active area for both theory and experiment. Substantial progress has been made in the application of HQE calculations to inclusive decays, with fits to moments of $\overline{B} \rightarrow X_c \ell \overline{\nu}_\ell$ and $B \rightarrow X_s \gamma$ decays providing precise values for $|V_{cb}|$ and m_b . However, the tension between the inclusive and exclusive $|V_{cb}|$ values highlights the need for further work.

Measurements of inclusive $\overline{B} \rightarrow X_u \ell \overline{\nu}_\ell$ decays have improved, and additional theoretical treatments and improved knowledge of m_b have strengthened our determination of $|V_{ub}|$. Further progress in these areas is possible, but will require higher-order radiative corrections from the theory and, in the case of $|V_{ub}|$, improved experimental knowledge of the $\overline{B} \rightarrow X_c \ell \overline{\nu}_\ell$ background. While there has been impressive progress in the past few years, new challenges will need to be overcome to achieve a precision below 5% on $|V_{ub}|$ from inclusive decays.

Progress in both $b \rightarrow u$ and $b \rightarrow c$ exclusive channels depends crucially on progress in lattice calculations. Here the prospects are good (see, *e.g.*, Ref. 133), since unquenched lattice simulations are now possible, although the ultimate attainable precision is hard to estimate.

The measurements of $\overline{B} \rightarrow \pi \ell \overline{\nu}_\ell$ have improved significantly, including the first reasonably precise determination of the q^2 dependence. The experimental input will continue to improve as B -factory data sets increase. Reducing the theoretical uncertainties to a comparable level will require significant effort, but is clearly vital in order to compare the extracted $|V_{ub}|$ with the one obtained from inclusive decays.

Both $|V_{cb}|$ and $|V_{ub}|$ are indispensable inputs into unitarity triangle fits. In particular, knowing $|V_{ub}|$ with a precision of better than 10% allows a test of CKM unitarity in the most direct way, by comparing the length of the $|V_{ub}|$ side of the unitarity triangle with the measurement of $\sin(2\beta)$. This comparison of a “tree” process ($b \rightarrow u$) with a “loop-induced” process ($B^0 - \overline{B}^0$ mixing) provides sensitivity to possible contributions from new physics. While the effort required to further

improve our knowledge of these CKM matrix elements is large, it is well motivated.

The authors would like to acknowledge helpful discussions with C. Schwanda, E. Barberio, F. Di Lodovico, V. Luth, A. Hoang, and I. I. Bigi.

References

1. R. Kowalewski and T. Mannel, J. Phys. **G33**, 1 (2006).
2. E. Barberio *et al.*, [arXiv:0704.3575](https://arxiv.org/abs/0704.3575).
3. N. Isgur and M.B. Wise, Phys. Lett. **B232**, 113 (1989); *ibid.*, **B237**, 527 (1990).
4. M.A. Shifman and M.B. Voloshin, Sov. J. Nucl. Phys. **47**, 511 (1988) [Yad. Fiz. **47**, 801 (1988)].
5. M.E. Luke, Phys. Lett. **B252**, 447 (1990).
6. M. Ademollo and R. Gatto, Phys. Rev. Lett. **13**, 264 (1964).
7. A.V. Manohar and M.B. Wise, Camb. Monogr. Part. Phys. Nucl. Phys. Cosmol. **10**, 1 (2000).
8. B. Grinstein, Nucl. Phys. **B339**, 253 (1990);
H. Georgi, Phys. Lett. **B240**, 447 (1990);
A.F. Falk *et al.*, Nucl. Phys. **B343**, 1 (1990);
E. Eichten and B. Hill, Phys. Lett. **B234**, 511 (1990).
9. C.G. Boyd, B. Grinstein, and R.F. Lebed, Phys. Rev. **D56**, 6895 (1997); *ibid.*, Phys. Rev. Lett. **74**, 4603 (1995);
C.G. Boyd and M.J. Savage, Phys. Rev. **D56**, 303 (1997).
10. I. Caprini *et al.*, Nucl. Phys. **B530**, 153 (1998).
11. A. Sirlin, Nucl. Phys. **B196**, 83 (1982).
12. A. Czarnecki and K. Melnikov, Nucl. Phys. **B505**, 65 (1997).
13. J. Laiho *et al.*, [arXiv:0710.1111](https://arxiv.org/abs/0710.1111); S. Hashimoto *et al.*, Phys. Rev. **D66**, 014503 (2002).
14. D. Buskulic *et al.* (ALEPH Collab.), Phys. Lett. **B395**, 373 (1997).
15. G. Abbiendi *et al.* (OPAL Collab.), Phys. Lett. **B482**, 15 (2000).
16. P. Abreu *et al.* (DELPHI Collab.), Phys. Lett. **B510**, 55 (2001).
17. J. Abdallah *et al.* (DELPHI Collab.), Eur. Phys. J. **C33**, 213 (2004).
18. N.E. Adam *et al.* (CLEO Collab.), Phys. Rev. **D67**, 032001 (2003).

19. B. Aubert *et al.* (BaBar Collab.), Phys. Rev. **D71**, 051502 (2005); updated in [arXiv:0705.4008](#).
20. B. Aubert *et al.* (BaBar Collab.), Phys. Rev. **D74**, 092004 (2006); updated in [arXiv:0705.4008](#).
21. B. Aubert *et al.* (BaBar Collab.), [arXiv:0707.2655](#).
22. B. Aubert *et al.* (BaBar Collab.), Phys. Rev. **D76**, 051101 (2007); updated in [arXiv:0708.1738](#).
23. D. Liventsev *et al.* (Belle Collab.), Phys. Rev. **D72**, 051109 (2005); updated in [arXiv:0711.3252](#).
24. N. Uraltsev, Phys. Lett. **B585**, 253 (2004).
25. M. Okamoto *et al.* Nucl. Phys. (Proc. Supp.) **B140**, 461 (2005). A. Kronfeld, talk presented at the workshop CKM05, San Diego, CA - Workshop on the Unitarity Triangle, 15-18 March 2005.
26. J.E. Bartelt *et al.* (CLEO Collab.), Phys. Rev. Lett. **82**, 3746 (1999).
27. K. Abe *et al.* (Belle Collab.), Phys. Lett. **B526**, 247 (2002).
28. S. Hashimoto *et al.*, Phys. Rev. **D61**, 014502 (2000).
29. G.M. de Divitiis, R. Petronzio, and N. Tantalo, JHEP **0710**, 062 (2007).
30. A.V. Manohar and M.B. Wise, Phys. Rev. **D49**, 1310 (1994).
31. I.I.Y. Bigi *et al.*, Phys. Rev. Lett. **71**, 496 (1993), Phys. Lett. **B323**, 408 (1994).
32. M.A. Shifman, [hep-ph/0009131](#), I.I.Y. Bigi and N. Uraltsev, Int. J. Mod. Phys. **A16**, 5201 (2001).
33. D. Benson *et al.*, Nucl. Phys. **B665**, 367 (2003).
34. M. Gremm and A. Kapustin, Phys. Rev. **D55**, 6924 (1997).
35. B.M. Dassinger, T. Mannel, and S. Turczyk, JHEP **0703**, 087 (2007).
36. I.I. Bigi, N. Uraltsev, and R. Zwicky, Eur. Phys. J. **C50**, 539 (2007).
37. P. Gambino and N. Uraltsev, Eur. Phys. J. **C34**, 181 (2004).
38. T. Becher, H. Boos, and E. Lunghi, [arXiv:0708.0855](#).
39. I.I.Y. Bigi *et al.*, Phys. Rev. **D56**, 4017 (1997).
40. I.I.Y. Bigi *et al.*, Phys. Rev. **D52**, 196 (1995).
41. A.H. Hoang *et al.*, Phys. Rev. **D59**, 074017 (1999).
42. H. Jautwyler, Phys. Lett. **B98**, 447 (1981); M.B. Voloshin, Sov. J. Nucl. Phys. **36**, 143 (1982).

43. C.W. Bauer *et al.*, Phys. Rev. **D70**, 094017 (2004).
44. S.E. Csorna *et al.* (CLEO Collab.), Phys. Rev. **D70**, 032002 (2004).
45. A.H. Mahmood *et al.* (CLEO Collab.), Phys. Rev. **D70**, 032003 (2004).
46. B. Aubert *et al.* (BaBar Collab.), Phys. Rev. **D69**, 111103 (2004); updated in [arXiv:0707.2670](https://arxiv.org/abs/0707.2670).
47. B. Aubert *et al.* (BaBar Collab.), Phys. Rev. **D69**, 111104 (2004).
48. C. Schwanda *et al.* (Belle Collab.), Phys. Rev. **D75**, 032005 (2007).
49. P. Urquijo *et al.* (Belle Collab.), Phys. Rev. **D75**, 032001 (2007).
50. J. Abdallah *et al.* (DELPHI Collab.), Eur. Phys. J. **C45**, 35 (2006).
51. D. Acosta *et al.* (CDF Collab.), Phys. Rev. **D71**, 051103 (2005).
52. P. Koppenburg *et al.* (Belle Collab.), Phys. Rev. Lett. **93**, 061803 (2004);
K. Abe *et al.* (Belle Collab.), [hep-ex/0508005](https://arxiv.org/abs/hep-ex/0508005).
53. B. Aubert *et al.* (BaBar Collab.), Phys. Rev. **D72**, 052004 (2005).
54. B. Aubert *et al.* (BaBar Collab.), [hep-ex/0507001](https://arxiv.org/abs/hep-ex/0507001).
55. S. Chen *et al.* (CLEO Collab.), Phys. Rev. Lett. **87**, 251807 (2001).
56. M. Battaglia *et al.*, Phys. Lett. **B556**, 41 (2003).
57. B. Aubert *et al.* (BaBar Collab.), Phys. Rev. Lett. **93**, 011803 (2004).
58. O. Buchmüller and H. Flächer, [hep-ph/0507253](https://arxiv.org/abs/hep-ph/0507253); updated in http://www.slac.stanford.edu/xorg/hfag/semi/LP07/gbl_fits/kinetic/lp07-update.pdf.
59. C.W. Bauer *et al.*, Phys. Rev. **D70**, 094017 (2004).
60. K. Abe *et al.* (Belle Collab.), [hep-ex/0611047](https://arxiv.org/abs/hep-ex/0611047).
61. See http://www.slac.stanford.edu/xorg/hfag2/semi/LP07gbl_fits/1S/index.html.
62. A. H. Hoang, Phys. Rev. **D61**, 034005 (2000), updated in [hep-ph/0008102](https://arxiv.org/abs/hep-ph/0008102).
63. K. Melnikov and A. Yelkhovsky, Phys. Rev. **D59**, 114009 (1999).
64. M. Neubert, [arXiv:0801.0675](https://arxiv.org/abs/0801.0675).
65. M. Neubert, [hep-ph/0506245](https://arxiv.org/abs/hep-ph/0506245).
66. A. H. Hoang *et al.*, Phys. Rev. **D59**, 074017 (1999).

67. N. Uraltsev, *Int. J. Mod. Phys.* **A14**, 4641 (1999).
68. M. Neubert, *Phys. Rev.* **D49**, 4623 (1994); *ibid.*, **D49**, 3392 (1994).
69. I. Bigi *et al.*, *Int. J. Mod. Phys.* **A9**, 2467 (1994).
70. B.O. Lange, M. Neubert, and G. Paz, *Phys. Rev.* **D72**, 073006 (2005).
71. C. W. Bauer *et al.*, *Phys. Lett.* **B543**, 261 (2002).
72. T. Mannel and S. Recksiegel, *Phys. Rev.* **D60**, 114040 (1999).
73. C.W. Bauer, Z. Ligeti, and M. E. Luke, *Phys. Rev.* **D64**, 113004 (2001).
74. C.W. Bauer *et al.*, *Phys. Rev.* **D68**, 094001 (2003).
75. S.W. Bosch *et al.*, *JHEP* **0411**, 073 (2004).
76. A.W. Leibovich *et al.*, *Phys. Lett.* **B539**, 242 (2002).
77. M. Neubert, *Phys. Lett.* **B543**, 269 (2002).
78. K.S.M. Lee and I.W. Stewart, *Nucl. Phys.* **B721**, 325 (2005).
79. M. Beneke *et al.*, *JHEP* **0506**, 071 (2005).
80. M. Neubert, *Phys. Lett.* **B513**, 88 (2001); *Phys. Lett.* **B543**, 269 (2002).
81. A.K. Leibovich *et al.*, *Phys. Rev.* **D61**, 053006 (2000); **D62**, 014010 (2000); *Phys. Lett.* **B486**, 86 (2000); **B513**, 83 (2001).
82. A.H. Hoang *et al.*, *Phys. Rev.* **D71**, 093007 (2005).
83. B. Lange *et al.*, *JHEP* **0510**, 084 (2005); B. Lange, *JHEP* **0601**, 104 (2006).
84. M. Neubert, *Phys. Lett.* **B612**, 13 (2005).
85. P. Gambino *et al.*, [hep-ph/0505091](#).
86. P. Gambino *et al.*, *JHEP* **0710**, 058 (2007).
87. J.R.Andersen and E. Gardi, *JHEP* **0601**, 097 (2006).
88. U. Aglietti *et al.*, [arXiv:0711.0860](#).
89. C.W. Bauer *et al.*, *Phys. Rev.* **D64**, 113004 (2001); *Phys. Lett.* **B479**, 395 (2000).
90. I.I.Y. Bigi and N.G. Uraltsev, *Nucl. Phys.* **B423**, 33 (1994).
91. M.B. Voloshin, *Phys. Lett.* **B515**, 74 (2001).
92. J.L. Rosner *et al.* (CLEO Collab.), *Phys. Rev. Lett.* **96**, 121801 (2006).
93. B. Aubert *et al.* (BaBar Collab.), [arXiv:0708.1753](#).
94. R. Barate *et al.* (ALEPH Collab.), *Eur. Phys. J.* **C6**, 555 (1999).

95. M. Acciarri *et al.* (L3 Collab.), Phys. Lett. **B436**, 174 (1998).
96. G. Abbiendi *et al.* (OPAL Collab.), Eur. Phys. J. **C21**, 399 (2001).
97. P. Abreu *et al.* (DELPHI Collab.), Phys. Lett. **B478**, 14 (2000).
98. A. Bornheim *et al.* (CLEO Collab.), Phys. Rev. Lett. **88**, 231803 (2002).
99. A. Limosani *et al.* (Belle Collab.), Phys. Lett. **B621**, 28 (2005).
100. B. Aubert *et al.* (BaBar Collab.), Phys. Rev. **D73**, 012006 (2006).
101. B. Aubert *et al.* (BaBar Collab.), Phys. Rev. Lett. **95**, 111801 (2005), Erratum-*ibid.* **97**, 019903(E) (2006).
102. R. Kowalewski and S. Menke, Phys. Lett. **B541**, 29 (2002).
103. B. Aubert *et al.* (BaBar Collab.), Phys. Rev. Lett. **92**, 071802 (2004), updated in [arXiv:0708.3702](https://arxiv.org/abs/0708.3702),.
104. I. Bizjak *et al.* (Belle Collab.), Phys. Rev. Lett. **95**, 241801 (2005).
105. B. Aubert *et al.* (BaBar Collab.), Phys. Rev. Lett. **96**, 221801 (2006).
106. See <http://www.slac.stanford.edu/xorg/hfag2/semi/LP07/home.shtml>.
107. H. Kakuno *et al.* (Belle Collab.), Phys. Rev. Lett. **92**, 101801 (2004).
108. V. Golubev, Y. Skovpen, and V. Luth, Phys. Rev. **D76**, 114003 (2007).
109. D. Benson *et al.*, Nucl. Phys. **B710**, 371 (2005).
110. B. Aubert *et al.* (BaBar Collab.), Phys. Rev. Lett. **90**, 181801 (2003).
111. C. Schwanda *et al.* (Belle Collab.), Phys. Rev. Lett. **93**, 131803 (2004).
112. N.E. Adam *et al.* (CLEO Collab.), Phys. Rev. Lett. **99**, 041802 (2007); Phys. Rev. **D76**, 012007 (2007); supercedes Phys. Rev. **D68**, 072003 (2003).
113. B. Aubert *et al.* (BaBar Collab.), Phys. Rev. **D72**, 051102 (2005).
114. E. Dalgic *et al.* (HPQCD), Phys. Rev. **D73**, 074502 (2006), Erratum-*ibid.*, **D75** 119906, 2007.
115. D. Becirevic and A.B. Kaidalov, Phys. Lett. **B478**, 417 (2000).

- 116. T. Becher and R.J. Hill, [hep-ph/0509090](#).
- 117. T. Becher and R.J. Hill, *Phys. Lett.* **B633**, 61 (2006).
- 118. M.C. Arnesen *et al.*, *Phys. Rev. Lett.* **95**, 071802 (2005).
- 119. T. Hurth *et al.*, [hep-ph/0509167](#).
- 120. M.A. Shifman, A.I. Vainshtein, and V.I. Zakharov, *Nucl. Phys.* **B147**, 385 (1979); *ibid.*, **B147**, 448 (1979).
- 121. P. Ball and R. Zwicky, *Phys. Rev.* **D71**, 014015 (2005).
- 122. G. Duplancic *et al.*, [SI-HEP2007-17](#).
- 123. P. Ball and R. Zwicky, *Phys. Rev.* **D71**, 014015 (2005).
- 124. N. Isgur and M.B. Wise, *Phys. Rev.* **D42**, 2388 (1990).
- 125. B. Grinstein and D. Pirjol, *Phys. Rev.* **D70**, 114005 (2004).
- 126. B. Aubert *et al.* (BaBar Collab.), *Phys. Rev. Lett.* **98**, 091801 (2007).
- 127. K. Abe *et al.* (Belle Collab.), *Phys. Lett.* **B648**, 139 (2007).
- 128. K. Abe *et al.* (Belle Collab.), [hep-ex/0610054](#).
- 129. B. Aubert *et al.* (BaBar Collab.), *Phys. Rev. Lett.* **97**, 211801 (2006).
- 130. D. Scora and N. Isgur, *Phys. Rev.* **D52**, 2783 (1995).
- 131. W. Brower and H. Paar, *Nucl. Instrum. Methods* **A421**, 411 (1999).
- 132. P. Ball, [arXiv:0705.2290](#); J.M. Flynn and J. Nieves, *Phys. Lett.* **B649**, 269 (2007); T. Becher and R.J. Hill, *Phys. Lett.* **B633**, 61 (2006); M. Arnesen *et al.*, *Phys. Rev. Lett.* **95**, 071802 (2005).
- 133. C.T.H. Davies *et al.* (HPQCD, MILC, and Fermilab Lattice Collab.), *Phys. Rev. Lett.* **92**, 022001 (2004).